

I. Tiseanu et al.

# **X-Ray Micro-Laminography for the Ex-Situ Analysis of W-CFC Samples Retrieved from JET ITER-Like Wall**

(18th May 2015 – 22nd May 2015)  
Aix-en-Provence, France

“This document is intended for publication in the open literature. It is made available on the clear understanding that it may not be further circulated and extracts or references may not be published prior to publication of the original when applicable, or without the consent of the Publications Officer, EUROfusion Programme Management Unit, Culham Science Centre, Abingdon, Oxon, OX14 3DB, UK or e-mail [Publications.Officer@euro-fusion.org](mailto:Publications.Officer@euro-fusion.org)”.

“Enquiries about Copyright and reproduction should be addressed to the Publications Officer, EUROfusion Programme Management Unit, Culham Science Centre, Abingdon, Oxon, OX14 3DB, UK or e-mail [Publications.Officer@euro-fusion.org](mailto:Publications.Officer@euro-fusion.org)”.

The contents of this preprint and all other EUROfusion Preprints, Reports and Conference Papers are available to view online free at <http://www.euro-fusionscipub.org>. This site has full search facilities and e-mail alert options. In the JET specific papers the diagrams contained within the PDFs on this site are hyperlinked.

# **X-ray micro-laminography for the ex-situ analysis of W-CFC samples retrieved from JET ITER-Like Wall**

I.Tiseanu<sup>1\*</sup>, T Craciunescu<sup>1</sup>, M. Lungu<sup>1</sup>, C. Dobrea<sup>1</sup> and JET contributors<sup>2</sup>

*EUROfusion Consortium, JET, Culham Science Centre, Abingdon, OX14 3DB, UK*

<sup>1</sup> *Nat. Inst. for Laser, Plasma and Radiation Physics, Bucharest, Romania*

<sup>2</sup> *See the Appendix of F. Romanelli et al., Proceedings of the 25th IAEA Fusion Energy Conference 2014, Saint Petersburg, Russia*

## **Abstract**

X-ray micro-laminography ( $\mu$ XCL) was qualified and implemented as a solution for the 3D microstructural analysis of W-CFC samples retrieved from JET ITER-Like Wall. As expected, the W layers spatially correlate with the morphology of the DMS780 CFC components, the PAN (polyacrylonitrile) fiber bundles and the neighboring felts. Depending on the position of the coating interface inside the composite material, three main cases were distinguished; (i) Tungsten layers coated parallel to PAN fiber bundles tend to have a quasi-continuous, weakly waved surface (waves amplitude  $<100 \mu\text{m}$ );(ii) Tungsten layers coated onto the relatively porous felt region appear to smoothly follow even the surface of the largest pores of around one quarter of mm and (iii) Samples coated perpendicular to the PAN fiber bundles display frequent and strong crater like discontinuities of the metal layer. The characteristics dimensions of these gaps range in the order of 300-400  $\mu\text{m}$  both in the coating plane and perpendicular to it. On some craters the bottom W layer is broken and the generated debris can be found even deeper than one mm into the CFC substrate. These W particles, sized of 20-40  $\mu\text{m}$ , are always found in the large vertical gaps located between the fiber bundles perpendicular on the coated surface.

Corresponding author: Ion Tiseanu, E-mail: tiseanu@infim.ro

## **Introduction**

In the current JET ITER-Like Wall (ILW) the divertor consists of tungsten coated CFC-tiles and one row of bulk tungsten. The need for fast and nondestructive methods for the 3D microstructural analysis of W-CFC samples retrieved from JET –ILW led us to develop a combined X-ray imaging technique based on X-ray micro-tomography ( $\mu$ XCT) and X-ray micro-laminography ( $\mu$ XCL). Unlike microscopy techniques, the X-ray imaging of plasma exposed samples could provide a reference overview of the coating structural integrity not hindered by inherent deposits or contaminants. This way tungsten thickness measurements conducted for erosion/deposition studies benefit from an educated selection of the sampling area of the surface for which the layer thickness is relevant. It also allow for a better management and interpretation of various surface (SEM, TEM, XPS) and depth profiling (SIMS, GDOES) analyses to be performed on the core samples.

In this study,  $\mu$ XCT was applied for the 3D visualization of the morphology of the JET type DMS780 CFC substrate.  $\mu$ XCL analysis was conducted for the coating structural integrity on selected JET-ILW cores samples ( $\Phi$ 7x10 mm) of tiles 1 to 8 (except tile 5) plus the HFGC tile exposed during 2011-2012 that have been specially prepared for depth profile studies. In addition, line profiles of the cumulative thickness of tungsten along the diameter of the core samples were measured in-situ by using an ad-hoc W K-line XRF method.

## **Materials and methods**

In JET-ILW the divertor coating nominal thicknesses are from 10-15  $\mu$ m for inner Tiles 3 and 4 up to 20-25  $\mu$ m for the outer Tiles 6, 7, 8 and Tile 1 (inner). A picture with JET divertor area and tiles identification is shown in Figure 1.

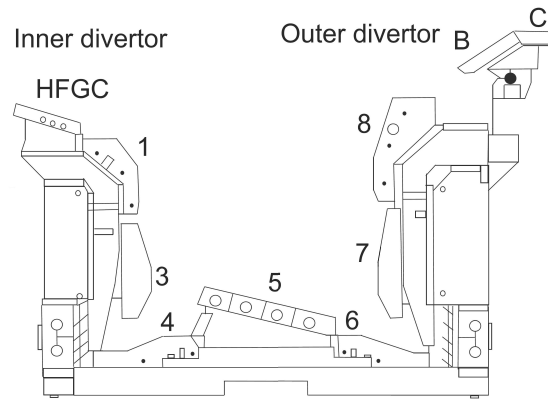


Fig. 1 JET divertor area and tiles identification

$\mu$ XCT is applied for the 3D visualization of the morphology of the CFC substrate. Figures 2 illustrates the morphology of JET type DMS780 CFC, a 2-D CFC formed by planes of PAN (polyacrylonitrile) fiber bundles perpendicularly oriented with interlayers (felt) of PAN fibers somehow randomly oriented. The minimum detectable feature is a single fiber of 6-7  $\mu\text{m}$  on a rather macroscopic sample of  $4 \times 4 \times 4 \text{ mm}^3$ . However, plain  $\mu$ XCT images of W-CFC core samples are affected by quite disturbing metal-induced streak artifacts due to the very strong X-ray attenuation along the multi-millimeter radiological path through tungsten coating.

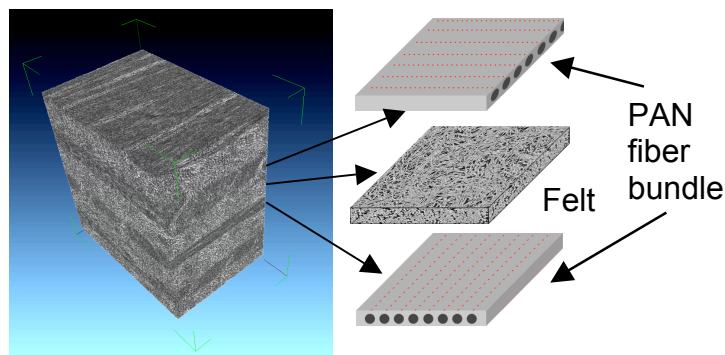


Figure 2: 3D tomography reconstruction of the DMS780 CFC with the main components composed of parallel PAN fiber bundles felt layers.

A better solution is to use X-ray micro-laminography ( $\mu$ XCL) that represents a generalization of  $\mu$ XCT [3]. This method permits the inspection of planar objects by using a

rotation axis tilted by less than 90 degrees with respect to the incident X-ray beam (Figure 3). Thus  $\mu$ XCL avoids using projections from angles closest to the sample coated surface leading thus to reconstructions with fewer artefacts. The most significant effect is represented by the increased contribution of the information containing X-ray interaction with the W coating as seen in the overall grey level histogram as depicted in the red circles of Figure 3.

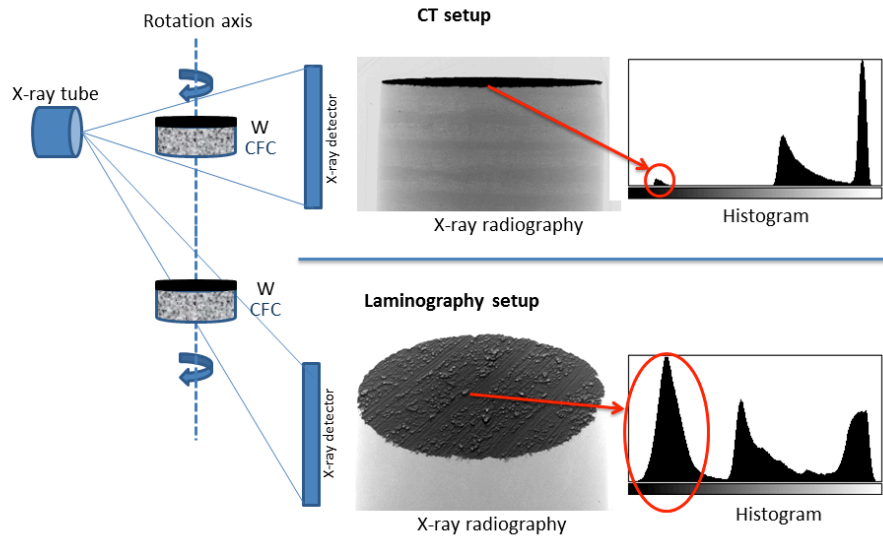


Figure 3: 3D micro-tomography versus X-ray micro-laminography scanning configurations

## Results and discussion

The  $\mu$ XCT/CL measurements were carried out at the X-ray microtomograph of INFLPR on selected JET-ILW cores samples from divertor tiles 1, 3, 4, 6, 7, 8 and HFGC (see Fig. 1) exposed during 2011-2012. The core samples (diameter of 7 mm) were tomographically inspected at a space resolution of  $\sim 3 \mu\text{m}$ ; obviously insufficient for an accurate W coating thickness measurement. Therefore, line profiles of the cumulative thickness of tungsten along the diameter of the core samples were measured in-situ by an ad-hoc W K-line XRF method. Based on the coating roughness shown on the  $\mu$ XCT/CL images we have estimated that a sampling area of  $1\text{-}2 \text{ mm}^2$  would be relevant for the layer thickness. Details of these works will be reported

elsewhere. Here, we note that from these absolute thickness measurements no significant erosion was detected on the investigated tiles in specific areas where the samples were cored from.

Composite Figure 4 illustrates the combined  $\mu$ XCT/CL imaging on a core sample of Tile 6. Tile 6 lies horizontally in the outer divertor (Figure 1) and was coated rigorously perpendicular to the PAN fiber bundles. Therefore samples retrieved from Tile 6 would present all possible coating/CFC interfaces to be representative for drawing a correlation of the W coating microstructural analysis versus CFC substrate morphology. As expected, the W layer follows the morphology of the DMS780 CFC PAN fiber bundles and felts. Tungsten layers coated parallel to PAN fiber bundles tend to have a quasi-continuous, weakly waved surface (waves amplitude  $<100 \mu\text{m}$ ). The relatively porous felt region is also relatively uniformly coated; the W layers display few moderate discontinuities with depths not exceeding quarter of mm that correspond to the largest pores. Coatings rigorously perpendicular to the PAN fiber bundles show frequent and strong crater-like discontinuities of the metal layer with characteristics dimensions of the discontinuities in the range of  $300\text{-}400 \mu\text{m}$  both in the coating plane and perpendicular to it. On some craters the bottom W layer is broken and this process generates debris that can be found even deeper than one mm into the CFC substrate. Typical size of those particles (most probable W) is approx.  $20\text{-}40 \mu\text{m}$ . It is likely that these particles were gravitationally trapped in these mm long and wide vertical gaps that exist along the fiber bundles perpendicular on the coated surface. JET plasma exposure surely played a role as we could not find such particle inclusions into freshly W coated CFC samples.

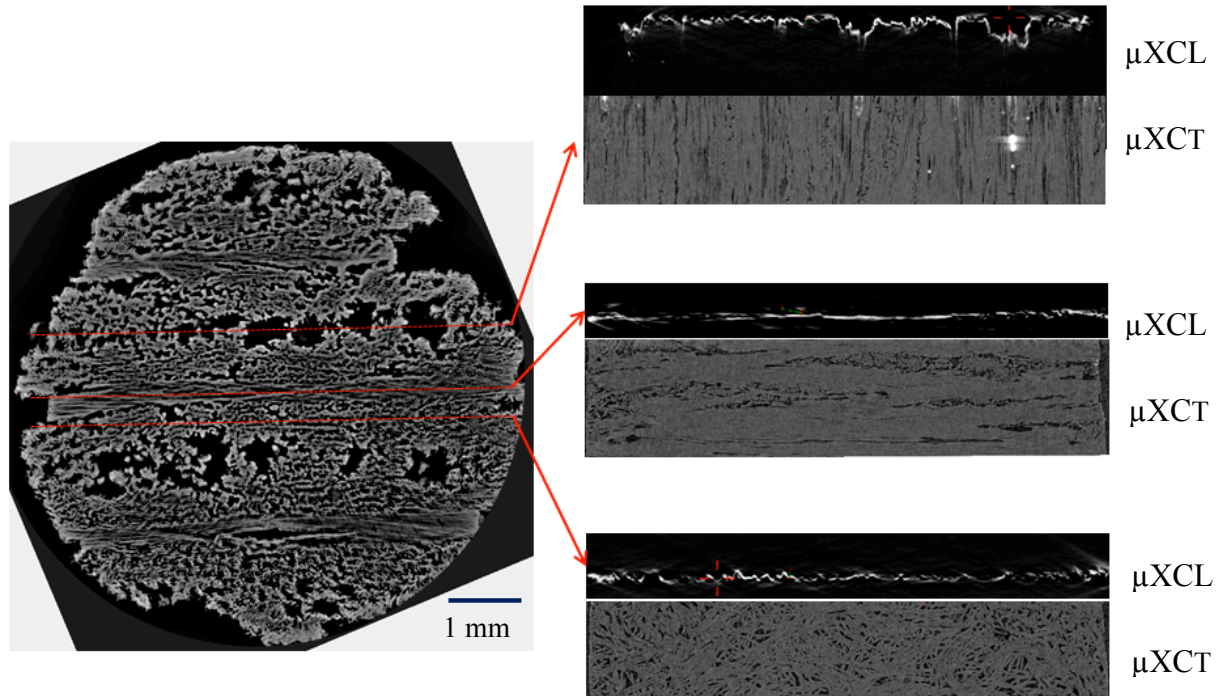


Figure 4:  $\mu$ XCT/CL imaging on a core sample of Tile 6. Left Panel:  $\mu$ XCL cross-section along the W coating layer. Right Panel: tomo/laminographic cross-sections along perpendicular planes passing through the dotted lines as follows: on top the PAN fiber bundles are oriented perpendicular on the coating; in the middle they are parallel to it and on bottom one shows a cross-section through a felt region. Each cross-section on the Right panel displays both the  $\mu$ XCL image of the W coating and the  $\mu$ XCT image of the CFC substrate.

Finally, we can speculate that there is the possibility that tokamak dust particles can follow the same mechanism to get infiltrated in some deep channels of the CFC tiles.



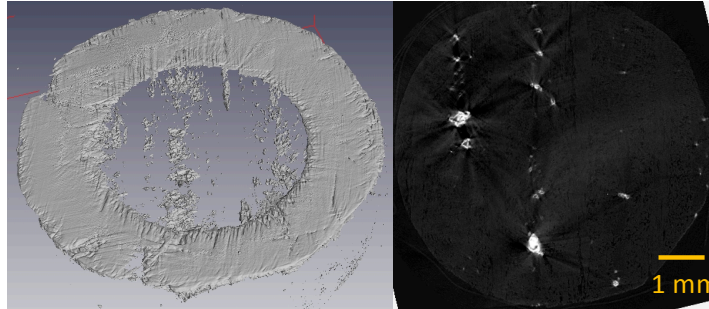


Figure 5: 3D representation of the remained W distribution after a GDOES analysis was performed until a depth of 65  $\mu\text{m}$  (left) and a tomographic cross-section taken at 200  $\mu\text{m}$  under the W layer.

The presence of a significant level of W inclusions under the nominal coating layer is likely to complicate the interpretation of any depth profile studies (for example by GDOES). We show in Figure 5 (Left), a 3D representation of the remained W distribution after a GDOES analysis that was performed until a depth of 65  $\mu\text{m}$  [4]. Figure 5 (Right) demonstrates the presence of relatively frequent W infiltrations even at a depth of 200  $\mu\text{m}$  measured from the W layer surface. One can note that same pattern of W structures is present both under the GDOES eroded and not-eroded region. A synthesis of the results obtained by studying the correlation between the W coating integrity versus the CFC substrate morphology is presented in Table 1.

Table 1: Synthesis of the qualitative microstructural analysis of selected core samples

Tile ID / no of core samples	Morphology of the coating interface	W thickness by HEXRF ( $\mu\text{m}$ )	Observations
1 / 2	perpendicular on PAN fiber bundles	$18.1 \pm 0.2$ $17.1 \pm 0.2$	Relatively smooth coating; rare crater-like structures along fiber bundles
3 / 3	at an angle of $\sim 80^\circ$ PAN fiber bundles	$18.9 \pm 0.2$ $16.8 \pm 0.2$ $18.5 \pm 0.2$	Moderately smooth coating; frequent crater-like structures with moderate depth along fiber bundles
4 / 2	rigorously perpendicular on PAN fiber bundles	$19.1 \pm 0.2$ $17.2 \pm 0.2$	Moderately smooth coating; frequent crater-like structures with moderate depth along fiber bundles

6 / 2	rigorously perpendicular on PAN fiber bundles	17.2 ± 0.2 18.2 ± 0.2	Coatings with affected structural integrity in form of deep crater-like structures and occasional delaminations
7 / 4	almost perpendicular on PAN fiber bundles	20.0 ± 0.2 19.4 ± 0.2 18.7 ± 0.2 17.5 ± 0.2	Coatings with frequent crater-like structures with moderate depth along fiber bundles
8 / 3	almost perpendicular on PAN fiber bundles	19.5 ± 0.2 20.5 ± 0.2 18.7 ± 0.2	Coatings with frequent crater-like structures with moderate depth along fiber bundles
HFGC / 3	rigorously parallel to the PAN fiber bundles	8.8 ± 0.3 9.1 ± 0.3 9.3 ± 0.3	Globally smooth coating appearance

Two general trends can be detected: i) coatings rigorously parallel to the PAN fiber bundles tolerate the tokamak plasma exposure without any microstructural change; ii) W coatings on the outer divertor are slightly more affected in terms of density and integral area of discontinuities than those on the inner tiles.

Only on two core samples of Tile 6 the coatings displayed somehow microstructural modifications in form of deep crater-like structures and occasionally delaminations.

## Conclusions

Herein, we proposed the combined X-ray micro-tomo/laminography as an effective method for the analysis of the microstructural integrity of the W-CFC samples retrieved from JET ITER-Like Wall. It is found that over a relevant number of samples, the W layers spatially correlated with the morphology of the DMS780 CFC substrates. We have also noticed that a significant level of W inclusions is present under the nominal coating layer that is likely to complicate the interpretation of any depth profile study (for example by GDOES). Line profiles of the cumulative thickness of tungsten along the diameter of the core samples were measured in-situ by an ad-hoc W K-line XRF method.

Finally, it is shown that, unlike microscopy techniques, X-ray imaging of plasma exposed samples could provide a reference overview of the coating structural integrity not hindered by deposits or contaminants.

### **Acknowledgments**

This work has been carried out within the framework of the EUROfusion Consortium and has received funding from the European Union's Horizon 2020 research and innovation programme under grant agreement number 633053. The views and opinions expressed herein do not necessarily reflect those of the European Commission.

### **References**

- [1] Tiseanu I. et al. Fusion Engineering and Design, Vol. 86, Issue 9-11, October 2011, Pages 1646-1651
- [2] Tiseanu I. et al. Physica Scripta, Volume T145, 014073, 5 pp. (2011).
- [3] Misawa, M, Tiseanu, I. Oblique-view cone-beam CT, US Patent 7139363 – 2006
- [4] C. Ruset et al., this conference